AD-A143 200 ASSOCIATION AND BOUND MOTION IN ALKALI METAL DOPED CADMIUM FLUORIDE(U) NAVAL ACADEMY ANNAPOLIS MD DEPT OF PHYSICS J J FONTANELLA ET AL. MAY 84 TR-12 1/1

UNCLASSIFIED F/G 7/4 NL

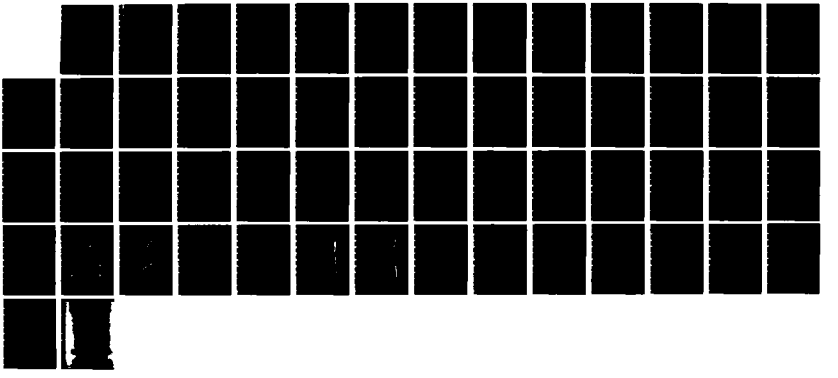

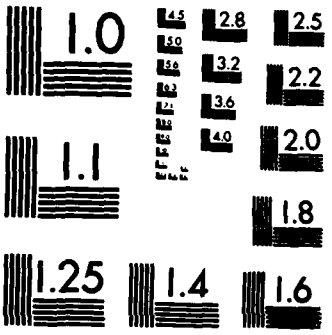

OFFICE OF NAVAL RESEARCH

Contract [redacted]

Task No. NR 627-793

TECHNICAL REPORT NO. 12

ASSOCIATION AND BOUND MOTION IN ALKALI METAL DOPED CADMIUM FLUORIDE

by

John J. Fontanella & Mary C. Wintersgill

Prepared for Publication

in

Journal of Physics C: Solid State Physics

U. S. Naval Academy
Department of Physics
Annapolis, MD 21402

May 1984

SECURITY CLASSIFICATION OF THIS PAGE (When Data Entered)

REPORT DOCUMENTATION PAGE		READ INSTRUCTIONS BEFORE COMPLETING FORM
1. REPORT NUMBER 12	2. GOVT ACCESSION NO.	3. RECIPIENT'S CATALOG NUMBER
4. TITLE (and Subtitle) ASSOCIATION AND BOUND MOTION IN ALKALI METAL DOPED CADMIUM FLUORIDE		5. TYPE OF REPORT & PERIOD COVERED Interim technical report 6. PERFORMING ORG. REPORT NUMBER
7. AUTHOR(s) JOHN J. FONTANELLA & MARY C. WINTERSGILL		8. CONTRACT OR GRANT NUMBER(s) ~~N0001484WR00001~~
9. PERFORMING ORGANIZATION NAME AND ADDRESS Physics Department U. S. Naval Academy Annapolis, MD 21402		10. PROGRAM ELEMENT, PROJECT, TASK AREA & WORK UNIT NUMBERS NR No. 627-793
11. CONTROLLING OFFICE NAME AND ADDRESS Office of Naval Research Attn. Code 413, 800 N. Quincy St. Arlington, VA 22217		12. REPORT DATE May 1984 13. NUMBER OF PAGES 47
14. MONITORING AGENCY NAME & ADDRESS(if different from Controlling Office)		15. SECURITY CLASS. (of this report) 15a. DECLASSIFICATION/DOWNGRADING SCHEDULE

16. DISTRIBUTION STATEMENT (of this Report)

Approved for public release and sale.
Distribution unlimited

17. DISTRIBUTION STATEMENT (of the abstract entered in Block 20, if different from Report)

18. SUPPLEMENTARY NOTES

19. KEY WORDS (Continue on reverse side if necessary and identify by block number)

Solid electrolytes, fluorine ion conductors, cadmium fluoride, alkali metals, electrical conductivity, electrical relaxation, high pressures

20. ABSTRACT (Continue on reverse side if necessary and identify by block number)

The effects of temperature and hydrostatic pressure on the ionic conductivity and the dielectric relaxation have been measured for lithium-, sodium-, and potassium-doped cadmium fluoride. Activation energies and activation volumes for the association region and for motion of the bound defects have been determined. These were found to depend strongly on the size of the dopant. For the nominally sodium doped material a single relaxation attributable to sodium is observed and is associated with NN fluorine vacancy-sodium substitutional pairs. For the potassium doped material, two distinct relaxations are observed,

DD FORM 1 JAN 73 1473 EDITION OF 1 NOV 65 IS OBSOLETE
S/N 0102-014-6601

SECURITY CLASSIFICATION OF THIS PAGE (When Data Entered)

Association and Bound Motion in Alkali Metal Doped Cadmium Fluoride

D.R. Figueroa
Universidad Simon Bolivar
Apartado 80659
Caracas, Venezuela

J.J. Fontanella and M.C. Wintersgill
Physics Department
U S Naval Academy
Annapolis Md. 21402, USA.

and

C. G. Andeen
Physics Department
Case Western Reserve University
Cleveland, Ohio 44106

which suggest the presence of both NN and NNN fluorine vacancy-potassium substitutional dipoles. A single relaxation peak is observed in the lithium doped material. It is attributed either to NN fluorine vacancy-substitutional lithium pairs or to lithium interstitial-lithium substitutional complexes. The activation energy for jumps of bound vacancies is largest for the sodium dopant for which the distortion is the least. The activation energies and the activation volumes for bound vacancy motion were found to be approximately in the same ratio as the values reported for free vacancy motion as expected from dynamical diffusion theories.

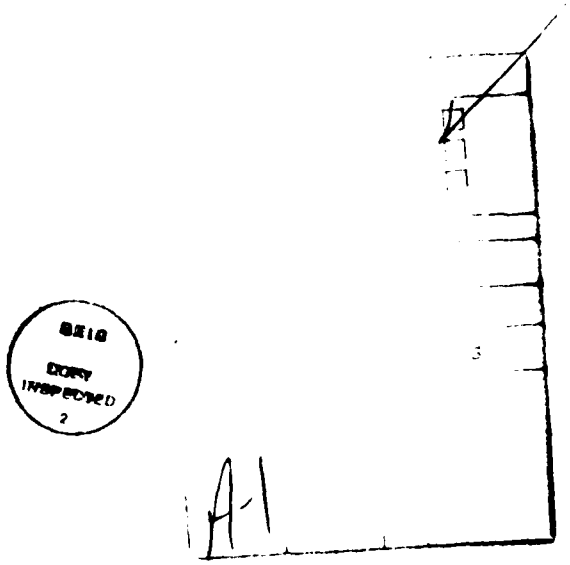

ABSTRACT

The effects of temperature and hydrostatic pressure on the ionic conductivity and the dielectric relaxation have been measured for lithium-, sodium-, and potassium-doped cadmium fluoride. Activation energies and activation volumes for the association region and for motion of the bound defects have been determined. These were found to depend strongly on the size of the dopant. For the nominally sodium doped material a single relaxation attributable to sodium is observed and is associated with NN fluorine vacancy - sodium substitutional pairs. For the potassium-doped material, two distinct relaxations are observed, which suggest the presence of both NN and NNN fluorine vacancy-potassium substitutional dipoles. A single relaxation peak is observed in the lithium doped material. It is attributed either to NN fluorine vacancy-substitutional lithium pairs or to lithium interstitial-lithium substitutional complexes. The activation energy for jumps of bound vacancies is largest for the sodium dopant for which the lattice distortion is the least. The activation energies and the activation volumes for bound vacancy motion were found to be in approximately the same ratio as the values reported for free vacancy motion as expected from dynamical diffusion theories.

I. INTRODUCTION

Cadmium fluoride is a fluorite-structured material that has received a good deal of attention since the discovery that it can be made an n-type semiconductor if doped with rare earths and heated in Cd vapor.[1] However, relatively little work has been devoted to the study of the ionic transport properties and at present very little is known concerning the nature and reorientation mechanism of bound defects.

When a monovalent impurity is introduced into these materials, a charge compensator is required. From density and lattice parameter measurements on CdF_2, Rubenstein and Banks[2] concluded that sodium ions Na^+ replace Cd^{2+} ions and charge compensation is achieved by the introduction of fluorine vacancies, F_v^-. In the case of the isostructural material CaF_2, which has a lattice constant (5.463 Å) very close to CdF_2 (5.388 Å), Johnson et al[3] also found, by internal friction and dielectric loss measurements, that Na^+ ions enter substitutionally and are compensated by F^- vacancies. However, theoretical calculations carried out by Franklin[4] predict that in CaF_2, substitution of Na+ ions on cation sites can be accompanied by either interstitial Na^+ ions or F^- vacancies. Another

possibility would be interstitial Na^+ ions accompanied by F^- interstitials. These configurations are shown in figure 1. More recent calculations of Jacobs et al[5] suggest that whether the M^+ ion will enter substitutionally and/or interstitially in CaF_2 will depend on the dopant. The corresponding defects for a variety of alkali-metal dopants in CaF_2 have been investigated by ionic-thermocurrent (ITC)[5] and dielectric relaxation (DR)[6] techniques. Only relaxation peaks attributable to substitutional M+ ions were observed. In SrF_2 and BaF_2 on the other hand, DR peaks were attributed both to substitutional $M^+ - F^-$ vacancy and to substitutional M^+ - interstitial M^+ complexes.[7] ITC techniques have been applied to Na - and Li-doped CdF_2 by Kunze and Muller[8] and to Na-doped CdF_2 by Kessler and Pflugger.[9] They report ITC peaks which were associated with impurity-vacancy dipoles, but a substantial discrepancy exists in the relaxation parameters they attribute to these peaks. The present work reports the results of the first study of the association and bound motion of M^+-F^- complexes by combined measurements of the effect of pressure and temperature on the ionic conductivity and dielectric relaxation in CdF_2. The purpose of this study is to

obtain an understanding of the defects formed when CdF_2 crystals are doped with alkali metal impurities covering an appropriate variety of ionic radii, Li(1.06 Å), Na(1.32 Å) and K(1.65 Å)[10].

II. EXPERIMENTAL TECHNIQUES

The crystals of undoped and alkali metal-doped cadmium fluoride were supplied by Optovac,Inc. All samples were cut into plates 1 cm^2 in area and 1 mm thick. The rough pieces were ground and lightly polished on fine-grit carborundum paper. Aluminum electrodes were prepared by vacuum evaporation onto opposite sides of the samples.

Capacitance and conductance measurements were carried out under vacuum, over the temperature range 5.5-300K. The measurements were carried out in a Cryogenics Associates CT-14 cryostat with an eight sample holder. Measurements as a function of pressure were made in a multiple sample holder, as described elsewhere.[11] Pressures up to 0.3 GPa. were generated using an Enerpac hand pump. The pressure cell was completely immersed in a fluid bath. Two different baths and pressure transmitting fluids were used. In the vicinity of room temperature, ethylene-glycol was

used in the bath and spinestic 22 oil was used as pressure fluid, whereas at low temperatures (160 K), freon was used in the bath and a 50:50 mixture of methanol and pentane was found more appropriate as the pressure fluid. The bath was stirred continuously and the temperature was controlled within $\pm$ 0.1 K

The data were taken at the five audio-frequencies: 10^2, $10^{2.5}$, 10^3, $10^{3.5}$ and 10^4 Hz using a fully automatic, microprocessor controlled bridge constructed by one of the authors (CGA). The bridge is operated through an Apple IIe microcomputer which is programed to take data at preset time intervals.

III. RESULTS AND DISCUSSION

A. TEMPERATURE DEPENDENCE OF THE IONIC CONDUCTIVITY

Conductivity measurements were limited to temperatures below room temperature. Higher temperatures were avoided since preliminary studies revealed some irreversible behavior after heating to 380 K. Typical conductivity curves of Log σT vs 1000/T are shown in figure 2 for CdF_2:Na. All data exhibit two different regions in this temperature interval, a frequency independent region (DC conductivity) and at least one dielectric loss peak

superimposed at lower temperatures. The dielectric loss is produced by dipole reorientation of defect complexes.

The DC conductivity data are well fitted by the Arrhenius function:

$$\sigma T = \sigma_0 \exp(-E/kT) \qquad (1)$$

where E is the activation enthalpy and σ_0 is a pre-exponential factor. The data and best-fit curves are shown in figure 3 and the best-fit values of σ_0 and E are given in Table 1. Included in that table are the activation energy values reported by Tan and Kramp[12] for the ionic conductivity in undoped and Na-doped CdF_2 in the region above room temperature. It is seen that the agreement with the present work is excellent.

The DC conductivity in the vicinity of room temperature is clearly due to charge carriers being thermally released from the associated defects. The Arrhenius parameters E and σ_0 can then be related to quantities involving the mobility of the charge carriers and the dissociation-association reaction for the complexes. It is assumed that the conductivity is due to fluorine vacancies and that the only defect reaction is:

$$M_s^+ + F_v^- \rightleftharpoons (M^+ - F^-)\text{pair} \qquad (2)$$

in which F_v^- denotes the free fluorine vacancy, M_s^+ the unassociated substitutional alkali metal and $(M^+ - F^-)$ the associated pair. The ionic conductivity is then given by:

$$\sigma = c_v N e \mu_v \qquad (3)$$

where c_v is the vacancy concentration (in mole fraction), μ_v is the mobility, e is the electronic charge and N the molecular density. The vacancy concentration is controlled by the dissociation reaction and is given by the mass-action law:

$$c_v c_s / c_p = (1/Z)\exp(-g_a/kT) \qquad (4)$$

in which g_a is the Gibbs-free energy of association ($g_a = h_a - Ts_a$, where h_a and s_a are the corresponding enthalpy and entropy). c_s and c_p are the concentrations (mol fraction) of unassociated substitutional cations and pairs respectively. Z is the number of equivalent orientations of the pair. Since F_v^- and M_s^+ are formed together, $c_v = c_s$ and if association is complete in this temperature region, $c_p >> c_v$ and $c_p \approx c$, the total impurity concentration (in mole fraction).

The concentration of free vacncies is then,

$$c_v = (c/Z)^{\frac{1}{2}} \exp(-g_a/2kT) \qquad (5)$$

The mobility is given by[13]

$$\mu_v = (e\ r^2 \nu_a/kT) \exp(-g_{fm}/kT) \qquad (6)$$

where r is the jump distance, ν_a is the attempt frequency and g_{fm} is the Gibbs-free energy for the free vacancy jump ($g_{fm}=h_{fm}-TS_{fm}$, where h_{fm} and S_{fm} are the enthalpy and entropy). Inserting Eqs. (5) and (6) into (3), the Arrhenius equation (1) is obtained. The activation energy E is given by

$$E = h_{fm} + \tfrac{1}{2} h_a \qquad (7)$$

and the pre-exponential factor σ_o is

$$\sigma_o = (c/Z)^{\frac{1}{2}} (Ne^2 r^2 \nu_a/k) \exp(S/k) \qquad (8)$$

where $S = s_{fm} + \tfrac{1}{2} s_a$

Using relation (7), the value of the adjusted parameter E can be used to obtain an association enthalpy h_a provided a value of h_{fm} is known.

The activation energy for free motion of vacancies is obtained from high temperature conductivity data. Unfortunately, at those temperatures the measurements are usually affected by sample contamination due to the high reactivity of

CdF_2. Tan and Kramp[12] obtained a value of 0.44 eV. However, they also pointed out that conductivity slopes as low as 0.35 eV were measured in the region of free motion (570K). Kessler and Caffyn[14] report a value of 0.51 eV from conductivity measurements. Measurements of diffusion coefficients of tracer ^{19}F have been carried out by Suptitz et al.[15] which yield a value of 0.39 eV for the enthalpy of vacancy motion in undoped and in sodium-doped CdF_2. The latter measurements would presumably be less sensitive to surface contamination.

In table 1, the association energies are calculated using the value of h_{fm} reported by Suptitz et al.[15] The choice of this value is supported by the result for sodium doped CdF_2 that h_{bm}=0.32 eV reported below since in the alkaline earth fluorides it is found that the activation energies for free vacancies are very close to the values for bound motion when the impurity is about the same size as the host cation.[6,7]

The general result is that the association energy tends to increase gradually with decreasing dopant ion size. It should be noted that this result is independent of the choice of h_{fm}. In support of the present model, then, are the theoretical calculations for the association energies of substitutional-vacancy complexes in CaF_2[5] which show this trend.

However, several other features of the conductivity results indicate that this model may need to be modified.

First, it is noted that the activation energy found for the undoped sample is larger than for the Na doped material and is approximately equal to that obtained for the lithium doped material. Next, it is observed that adding 0.01 mol% Na slightly decreases the conductivity of the "pure" CdF_2 while 0.1 mol% enhances the conductivity by a factor of about 12 at room temperature. More striking is the fact that doping CdF_2 with 0.1 mol% Li causes the conductivity to be depressed even more than for the 0.01 mol% Na sample.

The phenomena noted above can be explained as follows. The tracer diffusion measurements of Suptitz et al.[15] show that the conductivity of sodium doped CdF_2 is due to vacancies. Further, the dielectric relaxation results reported below show that the undoped cadmium fluoride contains at least 40 ppm sodium as a trace impurity in sodium substitutional-fluorine vacancy pairs and the 0.01 mol-% sample contains about 100 ppm sodium in the same complex. Since both the conductivity and activation energy in the undoped sample are higher than for the 0.01 mol% sample, it is concluded that the conductivity in the undoped material is at least in part due to undetected trace impurities. The conductivity is then lower in the deliberately doped sample because some of the sodium forms complexes with the known or unknown impurities which are then unable to release the charge carriers. The relatively small conductivity of the CdF_2:Li samples can, in part, be explained in the same way. In addition, it may be that the combination reaction:

$$Li_s^+ + Li_i^+ \rightleftharpoons (Li)_2 \qquad (9)$$

may be dominant in determining the charge carriers. If these complexes have a large binding energy, then the conductivity may be determined by the residual substitutional lithium-fluorine vacancy complexes, in which case the similarity between the activation energies of the undoped and Li doped samples is fortuitous. Alternatively, the conductivity may be controlled by the trace background impurities in which case the similarity in activation energies is automatic. However, as discussed below, it may be that predominantly substitutional lithium-fluorine vacancy complexes form where these complexes have an extraordinarily high binding energy. In this case, the conductivity will be controlled by the trace background impurities when the similarity in activation energies is once again automatic.

In the case of potassium, it is very unlikely, because of ion size, that the potassium ions will enter at interstitial sites. In this case a majority of substitutional impurities accompanied by fluorine vacancies would be expected. This model would explain the enhancement of ionic conductivity in the potassium doped samples.

IIIB. PRESSURE DEPENDENCE OF THE CONDUCTIVITY

The effect of pressure on the DC conductivity was determined in the association region. A typical example of the variation of the conductance divided by the frequency (G/ω) with pressure is shown in figure 4. It was found that $Ln(G/\omega)$ decreases approximately linearly as pressure increases. The data allow us to determine the activation volume associated with the conduction process. This is defined by the thermodynamic relation:

$$V = (\partial g/\partial P)_T \qquad (10)$$

where g is the Gibbs-free energy. Using the expression (1) for the conductivity, yields:

$$V = v_{fm} + \tfrac{1}{2} v_a = -kT\{\partial Ln\, \sigma /\partial P - \partial Ln\, \sigma_o/\partial P + (\partial S/\partial P)/k \} \qquad (11)$$

where v_{fm} is the activation volume for free vacancy motion and v_a is the association volume. The conductivity is related to the measured sample conductance by:

$$\sigma = \frac{Gt}{A} \qquad (12a)$$

where t and A are the sample thickness and area respectively. Then, it follows that:

$$\partial \mathrm{Ln}\,\sigma / \partial P = \partial \mathrm{Ln}G/\partial P + \chi_T/3 \qquad (12b)$$

where χ_T is the isothermal compressibility. After inserting equations (8) and (12) into (11) it follows that:

$$V = -kT\{\partial \mathrm{Ln}G/\partial P - \gamma_a \chi_T\} \qquad (13)$$

where γ_a is the Gruneisen parameter for the vibrational mode relevant to the jumping mechanism,

$$\gamma_a = -\left(\frac{\partial \mathrm{Ln}(\nu_a)}{\partial \mathrm{Ln}(V)}\right)_T \qquad (14)$$

Values of γ_a for cadmium fluoride are unknown, however, the activation volume is relatively insensitive to the value of γ_a , since the pressure dependence of G is by far the dominant contribution to V in equation (13). This small contribution can be estimated using the result of the dynamical diffusion theory of Flynn.[16]

$$V = 2\,\gamma_a \chi_T g \qquad (15)$$

Inserting the values of γ_a and χ_T given by equation (15) into equation (13) and neglecting the

entropy term, i.e. assuming g=E, we obtain for the activation volume:

$$V = -kT(\partial \ln G/\partial P)/(1-kT/2E) \qquad (16)$$

The resulting values calculated from this expression are listed in table 2.

This activation volume is taken as the sum of the migration volume V_{fm} and half an association volume $\frac{1}{2}V_a$. The activation volumes at high temperatures (above 500K) have been measured in CdF_2 by Oberschmidt and Lazarus.[19] They report a value of 3.1 $\pm$ 0.2 cm^3 /mol for the motion of free fluorine vacancies. If this value is subtracted from those calculated above, association volumes can be estimated for the different dopants in CdF_2. These are included in table 2. It is noted that the association volumes show a dependence on ionic radius similar to that found for the association enthalpies. These association volumes represent only a small fraction of the molar volume of CdF_2 (23.55 cm^3)

An interesting feature is that for the potassium dopant V_a is negative, although within the limits of the experimental errors it could be positive. A negative or zero activation volume is possible for

association of point defects. A migration volume on the other hand is expected always to be positive, if viewed as a lattice expansion accompanying the atomic jump. The association volume can be interpreted as the volume change of the lattice in bringing a vacancy, initially located at a remote position, into the immediate vicinity of the impurity. The net amount and direction of the lattice relaxation would depend then on the degree of distortion around the complex as compared with the distortion around the isolated defects. However, it is more likely that the value of V_{fm} reported by Oberschmidt and Lazarus is slightly too large, giving rise to an anomalous prediction of a negative value of V_a. In any event, the results indicate that the association volume is very sensitive to ion size.

III C. TEMPERATURE DEPENDENCE OF THE DIELECTRIC RELAXATION

Figure 5 shows the variation with temperature of the imaginary part of the dielectric constant ε'' for the series of 0.1 mol% AM-doped cadmium fluoride. It is seen that for each dopant different relaxations are present. For sodium, a single peak (163 K, 1000 Hz) is observed. For nominally lithium doped material, a main

peak is observed with a small relaxation superimposed on its high temperature tail. For the potassium doped material, the spectrum is composed of two closely spaced peaks and a weak peak at higher temperatures. The weak peak is common to the K- and Li-doped samples and is located at the same temperature as the peak in the Na-doped sample. This peak is attributed to traces of Na impurities present in the starting CdF_2 powder. This is verified by comparing the spectrum for undoped CdF_2 with those of CdF_2 doped with two different Na concentrations (0.01 mol% and 0.1 mol%) as illustrated in figure (6). The presence of residual Na impurities in CdF_2 is favored by the high solubility of NaF in CdF_2,[2] and partially explains the relatively high DC conductivity measured for the undoped sample. The concentration of sodium in the "pure" material can be estimated from the ratio of the peak intensities, $(c + c_o)/c$, where c_o is the background Na concentration and c is the added concentration. Almost the same number for c_o is obtained from the two doped samples (0.0042 and 0.0040 mol%).

The data were analyzed by fitting each peak with a broadened Debye curve using the Cole-Cole expression:[20]

$$\varepsilon'' = (A/2T)\cos(\alpha\pi/2)/\{\cosh((1-\alpha)x) + \sin(\alpha\pi/2)\} \quad (17)$$

where α is the Cole-Cole broadening parameter. A represents the strength of the dipole. Then

$$A = np^2/3\varepsilon_0 k \quad (17a)$$

where n is the dipole concentration, p is the dipole moment, and ε_0 is the permitivity of the free space.

$$x = Ln(\omega\tau) \quad (17b)$$

where τ is the most probable relaxation time and is given by

$$\tau = \tau_0 \exp(h_{bm}/kT) \quad (18)$$

Here τ_0 and h_{bm} are the reciprocal frequency factor and the activation enthalpy for the motion of bound vacancies, respectively. The fitting procedures are described elsewhere.[21] In the case of lithium, sodium was included in the fit by fixing the values of h_{bm}, τ_0, and α, and allowing A(K) to vary. Consequently, the small contribution of the background impurity was subtracted out. For the two potassium peaks, an expression containing two terms, that is a total of eight parameters, was fitted to the data. The data and best-fit curves are shown in figure 7 for potassium

doped cadmium fluoride. The best fit parameters obtained for all dopants are listed in table 3. Also included for comparison are the results reported by other workers using ionic thermo-current techniques. Compared to the present work, the value of E for the sodium peak reported by Kessler and Pflugger is lower by a factor of two, and their reciprocal frequency factor is extremely high. The activation energies reported by Kunze and Muller for the sodium and lithium peaks are in remarkable agreement with the present values. This comparison is very useful, since although ITC is a non-isothermal measurement, where a polarization discharge is heat-stimulated, it can be approximately regarded as a dielectric relaxation experiment at an extremely low frequency ($f \simeq 1.8 \times 10^{-3}$ Hz is estimated from the position of the sodium peak). The results for the sodium doped samples will be considered first. Several features imply that the peak is due to dipole relaxation associated with the reorientation of fluorine vacancies around the sodium ions. The strength of the relaxation increases with the sodium content whereas the temperature location and the relaxation parameters, h_{bm} and τ_0, do not depend upon the doping level. The sodium peak can be attributed to

motion of the NN fluorine vacancies along <100> directions adjacent to the substitutional sodium ions. This relaxation mode has been unambiguously identified in the case of Na-doped CaF_2[3] by comparison of dielectric and mechanical relaxation measurements. From the values of A obtained by peak fitting, the NN dipole concentration can be estimated, provided a value for the dipole moment p is assumed. For the unrelaxed point ion model: $p = ea_o\sqrt{3/2}$, where e is the electronic charge and a is the shortest anion-anion separation. The calculated concentrations are: c_D =.0097 mol% for the sample doped with 0.01 mol%Na and c_D =0.071 mol% for the sample doped with 0.1 mol%Na. Taking into account the additional background Na impurities, there is in each case a fraction of Na not forming vacancy-substitutional complexes. If it is assumed that the rest of the impurities are in the form of substitutional-interstitial complexes, the ratio of $(Na_s - Na_i)$ to $(Na_s - F_v)$ complexes in the 0.1 mol% sample is approximately 1/4.3. These calculations however, are based on two assumptions. First, the dopant concentration is taken as the nominal dopant concentration. The actual value should be determined by chemical analysis. Second, the undistorted point

ion model is used to calculate dipole moments. This is unrealistic, as lattice distortion is produced around the defects. If an appreciable population of substitutional-interstitial complexes do exist for the sodium doped samples, it may be that these complexes have a very large reorientation energy since no additional relaxation peaks were detected. Alternatively, it is possible that the absence of an additional peak could be due to a "split interstitial" configuration for the sodium ions which would have a negligible dipole moment.

For the lithium peak, a similar model, vacancy-impurity dipoles, can be used. In this case, the undistorted point ion model gives 0.063% for the concentration of lithium ions in substitutional-fluorine vacancy complexes. This is only slightly lower than that calculated for 0.1 mol% sodium samples. In fact, the similarity between the results for CdF_2:Li and CdF_2:Na and CaF_2:Li and CaF_2:Na[6] is quite striking and the slight differences are exactly that which is expected on the basis of the sizes of the host cations. However, as mentioned above, there is one serious difficulty with this model. In order to explain the low conductivity of CdF_2:Li, it is necessary for the substitutional-vacancy complexes to have a very large association energy. However, an alternative explanation is to attribute the relaxation to substitutional-interstitial lithium pairs. In support of this model, the concentration of dipoles that would represent the lithium peak is calculated to be 0.047 mol%, which would

correspond to 0.095 mol% lithium ions. This is very close to the nominal impurity concentration of 0.1 mol%. Further, theoretical calculations for CaF_2[5] show that in the case of the small lithium ion, this complex is favored over the substitutional-vacancy center. However, those calculations also showed that the structure of the complex is a non-dipolar (100) dumbbell, and thus it could not give rise to an electrical relaxation. It may be that the smaller lattice constant of CdF_2 gives rise to a dipolar substitutional-interstitial complex. However, in the event that such a complex is formed, it is difficult to imagine a reorientation mechanism by which lithium interstitials could move with an activation energy as low as 0.25 eV. Consequently, the situation for lithium doped CdF_2 is not clear.

For the potassium dopant, simple ion size considerations rule out the possibility of potassium interstitials. Thus, the more likely mode of solution for the potassium dopant is replacing cadmium cations and

generating fluorine vacancies as charge compensators. If both potassium peaks are assigned to vacancy-impurity complexes, then either there are two different types of complexes or only one complex with two alternative reorientation mechanisms. The computer calculations for CaF_2[5] show that both nearest-neighbor (NN) and next-nearest-neighbor (NNN) complexes have considerable stability but that the NN is more stable. Also, it is found that of the two possible vacancy jump directions for the NN, <100> and <110>, the former is favored. In addition, the calculations suggest that the reorientation energies for the NNN would be lower than for the NN. On the basis of the relative intensities and activation energies the weaker peak (with lower activation energy) can be assigned to NNN vacancy-potassium complexes and the more intense to NN complexes. However, the calculated total dipole concentration (NN plus NNN) only amounts to about one third of the total impurity concentration. One possible explanation for this difference is that potassium is not as soluble as sodium in CdF_2 and part of the potassium dopant added during growth remains precipitated. This might also explain why the conductivity for 0.1 mol% potassium falls below that

for the same concentration of sodium.

Finally, the results are consistent with previous results for alkali metal doped alkaline earth fluorides, in that the largest activation energy, h_{fm}, is observed for the dopant (Na) whose size most closely matches that of the host cation. Further, that activation energy (0.32 eV) is close to that for the motion of free vacancies (0.39-0.51 eV). This represents further evidence that the effects of distortion are to decrease the activation energies.

IIID. PRESSURE DEPENDENCE OF THE DIELECTRIC RELAXATION

Pressure data were taken isothermally at two different temperatures in the vicinity of the sodium peak. It is found that the peak position shifts to lower frequencies with the application of pressure, as shown in figure 8. The $Ln(G/\omega)$ vs pressure data at fixed temperature and pressure were analysed as a function of frequency by fitting the Cole-Cole expression:

$$G/\omega = (B/2)\cos(\alpha\pi/2)/\{\cosh((1-\alpha)x) + \sin(\alpha\pi/2)\} \quad (19)$$

All quantities in Eq (19) have the same meaning as in equation (17) and B is a constant. Typical data and best-fit curves are shown in figure 8. At the peak

position $\omega\tau = 1$. This condition enables us to obtain directly the relaxation time τ at each pressure. Figure 9 shows the plot of $\mathrm{Ln}\,\tau$ against pressure. The activation volume for bound vacancy motion can be calculated from the pressure derivative of $\mathrm{Ln}\,\tau$. Starting from equation (10) with g being the Gibbs free energy for bound motion, and using the notation of Nowick[22] to relate the relaxation time to the approach frequency,

$$\tau = (1/2\nu_a)\exp(g_{bm}/kT) \qquad (20)$$

we obtain,

$$v_{bm} = kT\,\{\partial \mathrm{Ln}\,\tau/\partial P + \gamma_a \chi_T\} \qquad (21)$$

which is similar to expression (13). The actual attempt mode for bound vacancy motion is not known, however as in the case of the conductivity, the values of γ_a and χ_T are not very important for the calculation of v_{bm}, as the second term in this equation amounts at most to 3% of the first term. However, for the purpose of this calculation, dynamical diffusion theory[16] was used to obtain the working equation:

$$v = kT\,(\partial \mathrm{Ln}\,\tau/\partial P)/\{1 - kT/2h_{bm}\} \qquad (22)$$

where h_{bm} is the enthalpy for bound motion. The

values of the activation volumes calculated from this expression are listed in table 4. Indeed, the activation volume for bound vacancy motion, V=2.6-2.9cm^3/mol, is somewhat larger than that reported for CaF_2:Na (1.73 cm^3/mol). This difference is reasonable since the lattice constant is smaller for CdF_2, and consequently volume changes in the crystal due to the motion of a given diffusing species would be expected to be larger in CdF_2. Further, the activation volumes and activation energies for bound vacancy motion may be compared with the corresponding values for free vacancy motion. Assuming the value of h_{fm}=0.39eV as reported by Suptitz et al.[15] and the value v_{fm}=3.1 cm /mol of Oberschmidt and Lazarus[19] it is found that the ratio of activation energies h_{bm}/h_{fm}= 0.83 is approximately the same as the ratio of activation volumes, v_{bm}/v_{fm} = 0.85. A similar result is found for the alkaline earth fluorides. This relationship has also been found in the AEF and is expected on the basis of dynamical diffusion theory or similar models.[23] However, this result is remarkable, considering the fact that the present measurements were carried out at low temperatures (160K) whereas free vacancy motion occurs above 500K. In this high temperature regime, the vacancies are jumping several orders of magnitude faster than in the case of bound vacancy motion.

Next, it is noted that the activation volume decreases as temperature increases. This result has been noted previously for bound complexes in alkali metal doped alkaline earth fluorides.[24,25] An explanation is given elsewhere.[24]

Finally, a few comments are appropriate concerning the attempt mode Gruneisen parameter, γ_a. In previous papers which were concerned with alkali metal doped alkaline earth fluorides,[25] γ_a for vacancies was successfully approximated by the Raman mode, γ_R, particularly when the size of the alkali metal is the same as the alkaline earth. For CdF_2:Na, however, it does not appear that this approximation is valid. Specifically, using the calculated activation volume in equation (15) requires a value of γ_a=3.9. This is substantially larger than the measured value for the Raman mode, γ_R=1.4.[17] The most likely explanation for the failure is that because CdF_2 has a small lattice constant, the distortions associated with the local transport (attempt) mode are so large, that the approximation to a lattice mode is invalid.

IV. CONCLUSIONS

From measurements of electrical conductivity and relaxation at high pressures, several important features concerning the defect complexes in CdF_2 can be observed:

i. The conductivity in the association region can be interpreted in terms of the incorporation of alkali-metal ions in the CdF_2 matrix at normal cation sites or at interstitial positions, depending on the ionic radius of the impurity. It appears that for sodium and potassium the preferred mode of solution is a substitutional cation-anion vacancy complex. The situation is not so clear for lithium. It may be that for the smaller lithium ions, a cation substitutional-cation-interstitial complex is preferred.

ii. A single relaxation peak was observed in the sodium doped samples. This was associated with the motion of NN fluorine vacancies around substitutional sodium ions. For the potassium doped material the existence of two peaks is explained by the presence of NN and NNN fluorine vacancy-potassium substitutional complexes. The peak observed for lithium is attributed either to the motion of lithium interstitials adjacent to lithium substitutional ions or to the motion of NN fluorine vacancies around substitutional lithium ions.

iii. The trends in the variation of the

activation energies with impurity sizes are very similar to those for the activation volumes, in that all energies and volumes are larger for the smaller cations.

iv. The activation energy for bound vacancy motion was found to be greatest for the sodium doped CdF_2, and this value is closest to the activation energy for free vacancy motion. This indicates that the lattice distortion, due to mismatch in ion size between the dopant and the host cation, reduces the potential energy barrier for reorientation. This agrees with previous results in the alkaline earth fluorides.

v. The activation volume is found to scale with the Gibbs energy in good agreement with theory and with previous results in the alkaline earth fluorides.

ACKNOWLEDGMENTS

This work was supported in part by the Office of Naval Research.

REFERENCES

(1) J. D. Kingsley and J. S. Prener, Phys. Rev. Letters, 8, 315 (1962).

(2) M. Rubenstein and E. Banks, J. Electrochem. Soc. 106, 404 (1959).

(3) H. B. Johnson, N. J. Tolar, G. R. Miller, and I. B. Cutler, J. Phys. Chem. Solids, 30, 31 (1969).

(4) A. D. Franklin, J. Amer. Ceram. Soc. 50, 648, (1967).

(5) P. W. M. Jacobs, S. H. Ong, A. V. Chadwick, and V. M. Carr, J. Solid State Chem. 33, 159 (1980).

(6) J. J. Fontanella, A. V. Chadwick, V. M. Carr, M. C. Wintersgill and C. G. Andeen, J. Phys. C:Solid St. Phys. 13, 3457 (1980).

(7) M. C. Wintersgill, J. J. Fontanella, R. Saghafian, A. V. Chadwick , and C. G. Andeen, J. Phys. C: Solid St. Phys. 13, 6525 (1980).

(8) I. Kunze and P. Muller, Phys. Sta. Solidi (a), 13, 197 (1972).

(9) A. Kessler and R. Pflugger, J. Phys. C: Solid St.

Phys. 11, 3375 (1978).

(10) R. D. Shannon, Acta Crystallogr. A32, 751 (1976).

(11) J. J. Fontanella, C. G. Andeen, and D. Schuele, Phys. Rev. B6, 582 (1972).

(12) Y. T. Tan and D. Kramp, J. Chem. Phys. 53, 3691 (1970).

(13) A. B. Lidiard, Hand. d. Physik, 20, 246 (1957).

(14) A. Kessler and J. E. Caffyn, J. Phys. C: Solid St. Phys. 5, 1134 (1972).

(15) P. Suptitz, E. Brink, and D. Becker, Phys. Stat. Solidi (b) 54, 713 (1972).

(16) C. P. Flynn, Point Defects and Difussion (Clarendon, Oxford, 1972)

(17) J. R. Kessler, E. Monberg, and M. Nicol, J. Chem. Phys. 60, 5057 (1974).

(18) C. G. Andeen, D. Schuele, and J. J. Fontanella, Phys. Rev. B6, 591 (1972).

(19) J. Oberschmidt and D. Lazarus, Phys. Rev. B21, 5823 (1980).

(20) C. P. Smyth, Dielectric behaviour and Structure (Mc-Graw-Hill, New York, 1955).

(21) R. J. Kimble Jr, P. J. Welcher, J. J. Fontanella, M. C. Wintersgill and C. G. Andeen, J. Phys. C:Solid State Physics 15, 3441 (1982).

(22) A. S. Nowick, Adv. Phys. 16, 1 (1967).

(23) P. Varotsos and K. Alexopoulos, J. Phys. Chem. Solids 42, 409 (1981).

(24) J. J. Fontanella, M. C. Wintersgill, and C. Andeen, Phys. Stat. Sol. (b)97, 303 (1980).

(25) J. J. Fontanella, M. C. Wintersgill, A. V. Chadwick, R. Saghafian, and C. G. Andeen, J. Phys. C: Solid State Physics 14, 2451 (1981).

TABLE 1 - Activation parameters for the DC conductivity in the association region of alkali metal-doped CdF_2.

Crystal	E(eV)	$Ln\sigma_o$ (Ω^{-1} cm^{-1} K)	h_a(eV)
undoped	0.715	14.34	0.65[b]
Tan and Kramp[a]	0.69		
Lithium (0.1 mol%)	0.715	13.74	0.65[b]
Sodium (0.01 mol%)	0.679	12.61	0.58
Sodium (0.1 mol%)	0.671	15.06	0.56
Tan and Kramp[a]	0.66		
Potassium (0.1 mol%)	0.628	11.86	0.48

a. Reference 12

b. Included for the purpose of comparison. See text.

TABLE 2 - Best fit parameters describing the conductivity as a function of pressure and activation volumes for alkali-metal doped cadmium fluoride

Crystal	T(K)	$-\frac{dLnG}{dP}$ (GPa^{-1})	V(cm^3/mol)	V_a(cm^3/mol)
Undoped	291	1.618	3.99	1.78[a]
	285	1.628	3.92	1.64[a]
Lithium (0.1 mol%)	291	1.655	4.08	1.96[a]
	285	1.616	3.90	1.60[a]
Sodium (0.1 mol%)	291	1.597	3.94	1.68
	285	1.64	3.96	1.72
Potassium (0.1 mol%)	291	1.226	3.03	-0.14
	285	1.238	2.99	-0.22

a. Included for the purpose of comparison. See text.

TABLE 3 - Activation parameters for the relaxation peaks in alkali metal doped CdF_2

Crystal	h_{bm}(eV)	$\tau_o(10^{-14}s)$	A(K)	α	rms error
Lithium (0.1 mol%)	0.251	8.47	61.27	0.069	0.021
Kunze and Muller[8] (ITC)	0.26	3.62			
Sodium (0.01 mol%)	0.322	1.62	9.47	0.061	0.014
Sodium (0.1 mol%)	0.323	1.49	69.3	0.028	0.007
Kunze and Muller[8] (ITC)	0.31	7.66			
Kessler and Pflugger[9] (ITC)	0.15	10^6			
Potassium (0.1 mol%)	0.128	45.3	8.26	0.021	0.005
	0.18	25.2	24.9	0.013	0.005

TABLE 4 - Best fit parameters describing the relaxation time as a function of pressure and activation volumes for vacancy bound motion in Na-doped CdF_2

Crystal	T(K)	$\frac{dLn\tau}{dP}$ (GPa^{-1})	V_{bm} (cm^3/mol)
CdF_2:0.1 mol% Na	161	1.972	2.69
	169	1.809	2.60

FIGURE CAPTIONS

FIGURE 1. Representation of possible configurations for univalent ions and the associated charge - compensating defects in the fluorite lattice.

Open circles - divalent cations M^{2+}
Solid circles - univalent impurity ions M^{+}
Cross hatch (grey) circles - fluorine ions F^{-}
Cube - fluorine vacancy F_v^{-}

FIGURE 2. Log ($\sigma T((\Omega^{-1} cm^{-1} K))$ against $1000/T(K^{-1})$ for 0.1 mol% sodium-doped cadmium fluoride. The lines connect the datum points and the curves from bottom to top are at 10^2, $10^{2.5}$, 10^3, $10^{3.5}$, and 10^4 Hz.

FIGURE 3. Log (σT $(\Omega^{-1} cm^{-1} K)$) against $1000/T$ (K^{-1}) for undoped and alkali-metal doped CdF_2.

FIGURE 4. Ln (G/ω (pF)) versus pressure (GPa) for 0.1 mol% potassium doped CdF_2. The datum points are shown along with the best straight line. O decreasing pressure; X increasing pressure.

FIGURE 5. ε'' versus temperature at 1000 Hz for alkali-metal-doped cadmium fluoride.

FIGURE CAPTIONS

FIGURE 6. ε'' versus temperature at 1000 Hz for undoped and sodium doped cadmium fluoride. Note that the ε'' values for the undoped and the 0.01 mol% doped samples have been multiplied by a factor of 4.

FIGURE 7. Data and best fit curves for ε'' versus temperatures for 0.1 mol% potassium-doped cadmium fluoride. Only the curves for the frequencies 10^2, 10^3 and 10^4 Hz are shown.

FIGURE 8. G/ω (pF) versus Ln f(Hz) for the sodium peak at two different pressures.

FIGURE 9. $\mathrm{Ln}(\tau(s))$ versus pressure (GPa) for the sodium peak at two different temperatures.

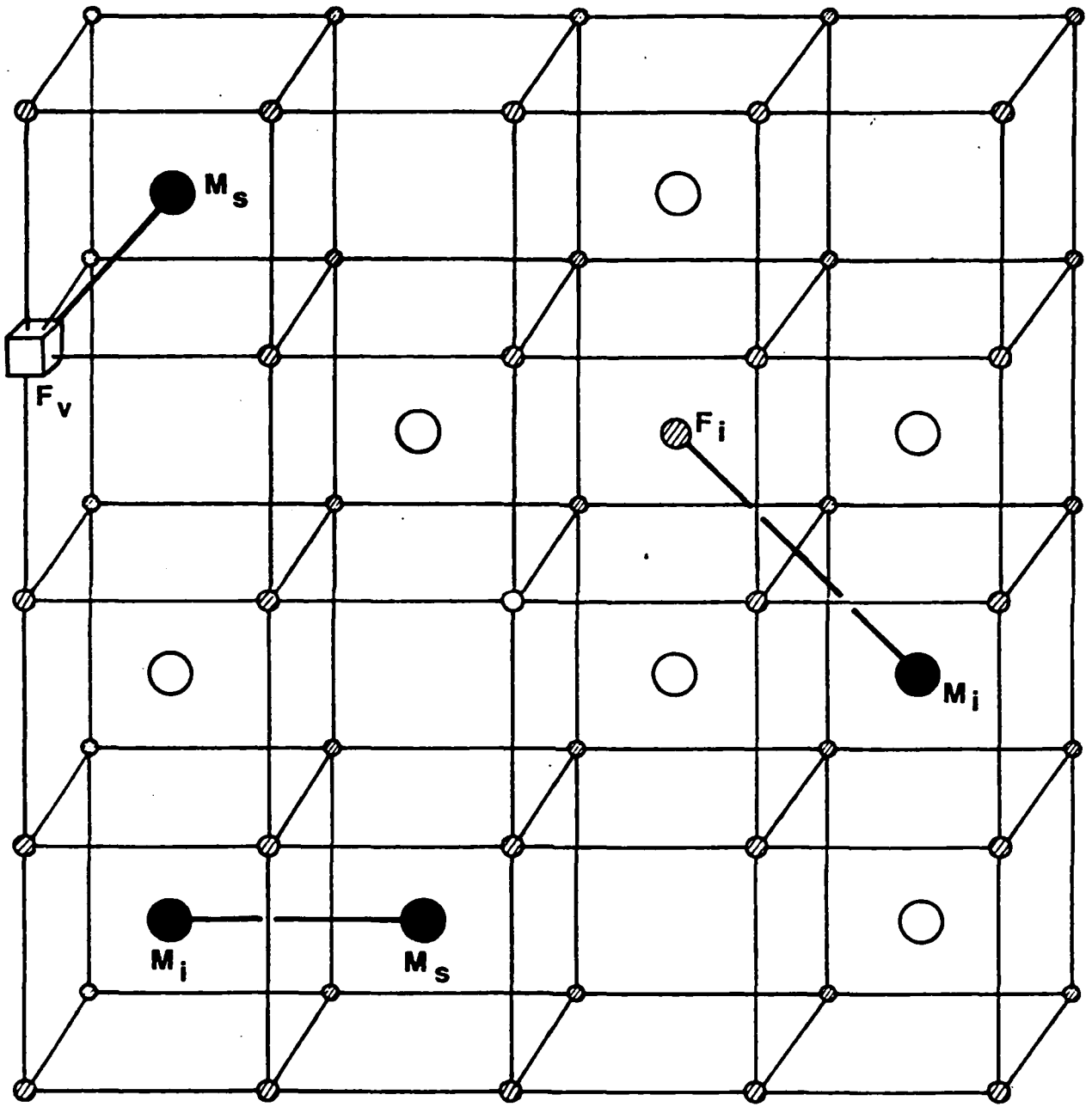
M_s
F_v
F_i
M_i
M_i
M_s

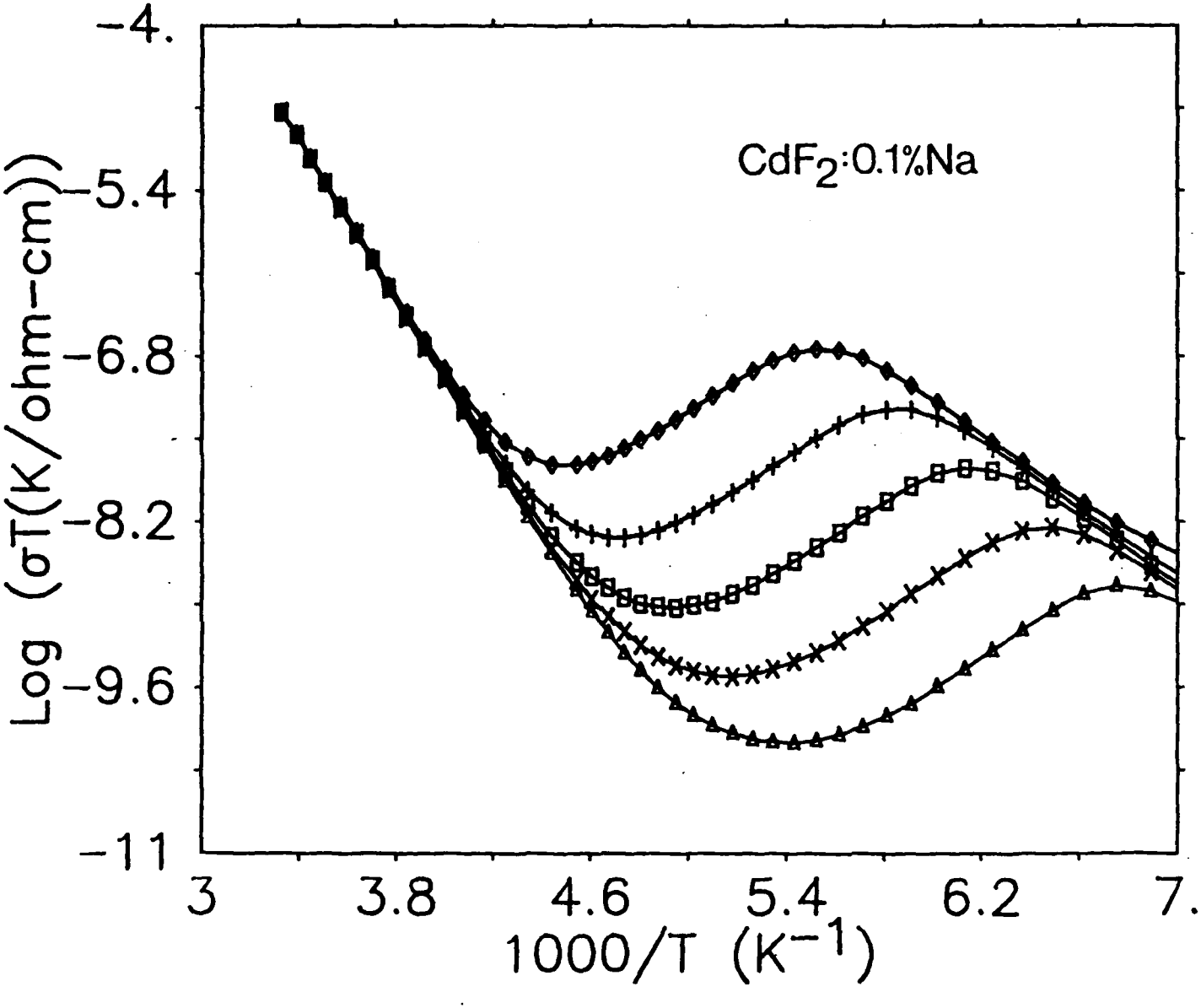

J. 2 - Figueroa et al.

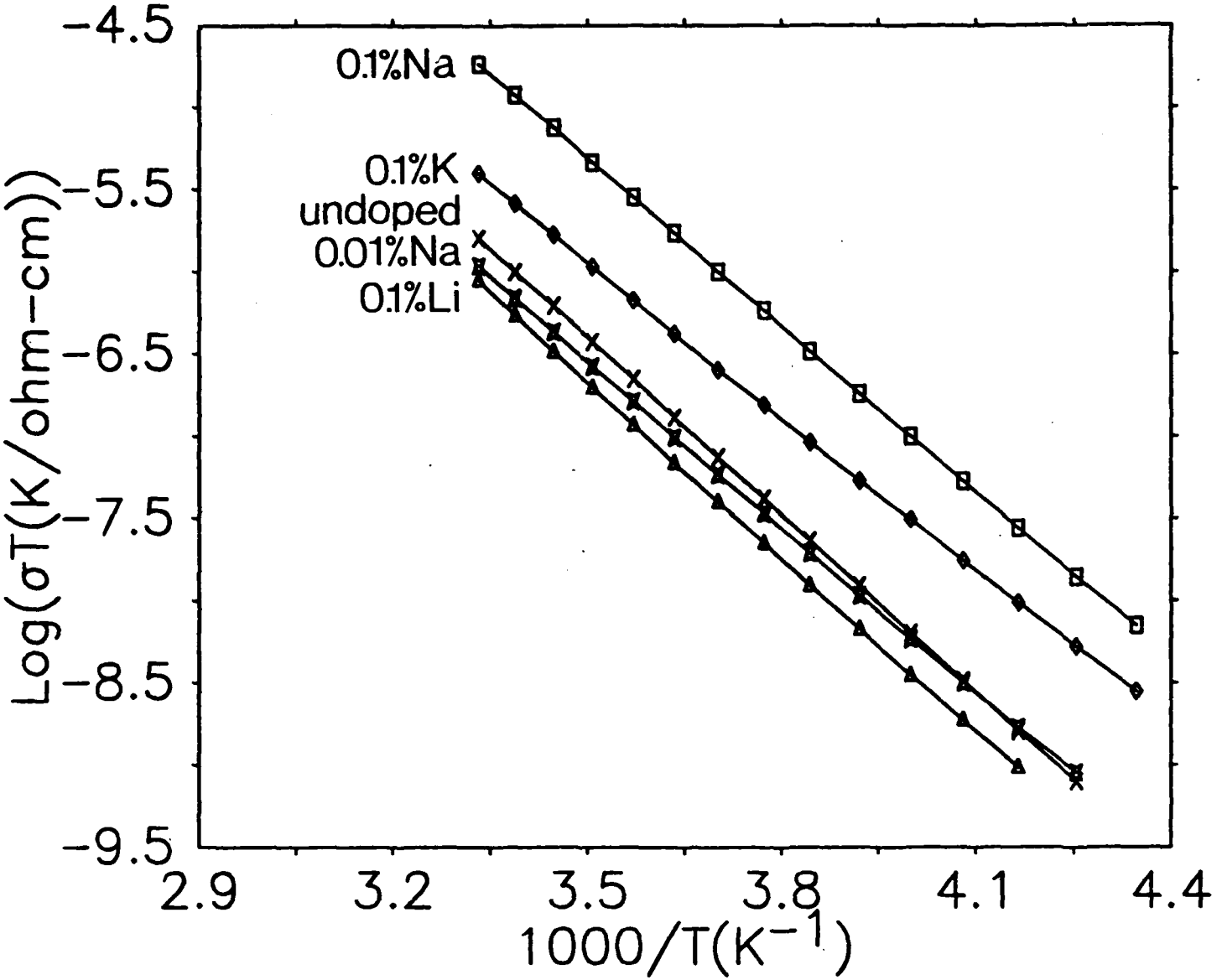

Fig. 3 - Figueroa et al

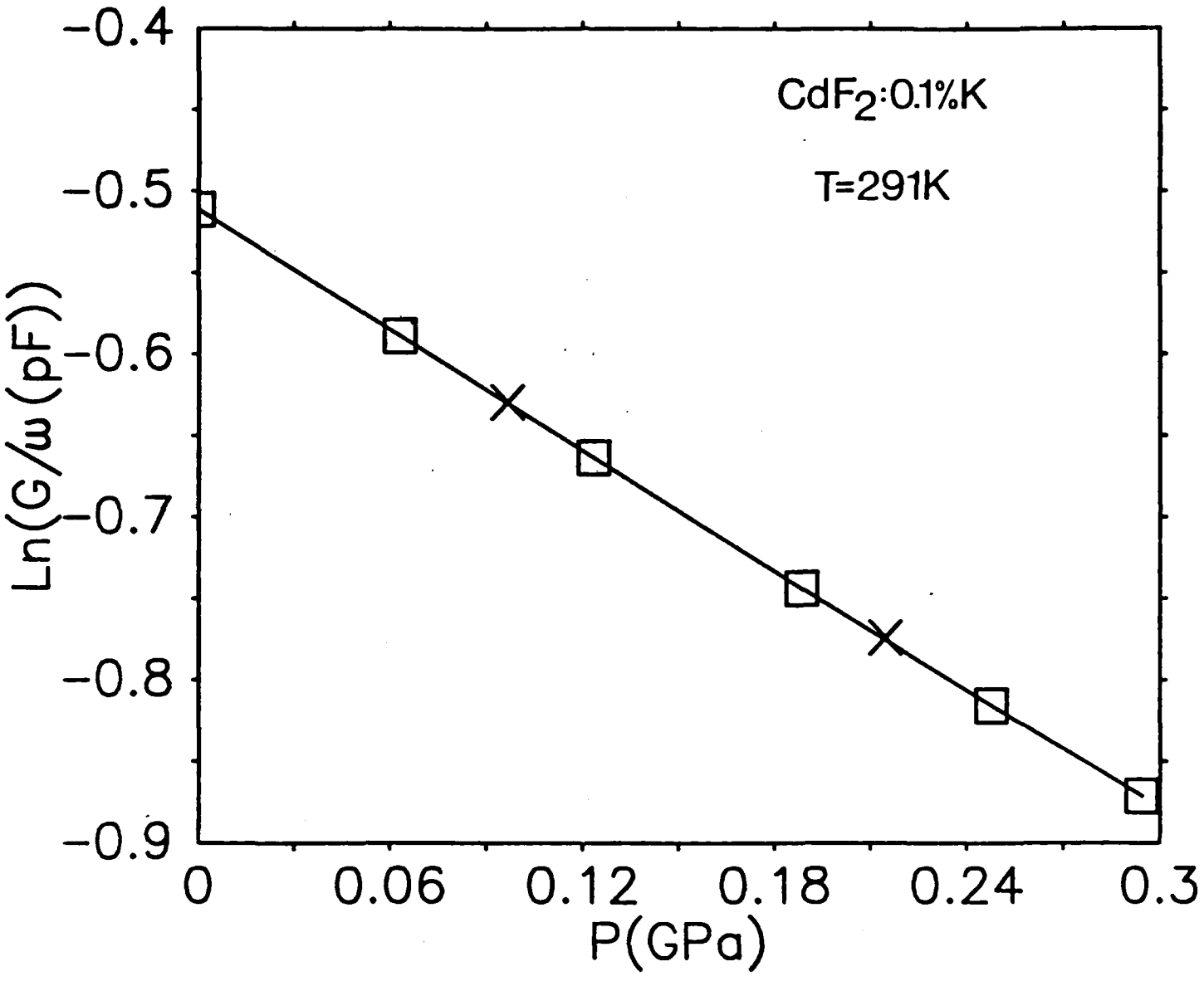

p. 4 - Figueroa et al.

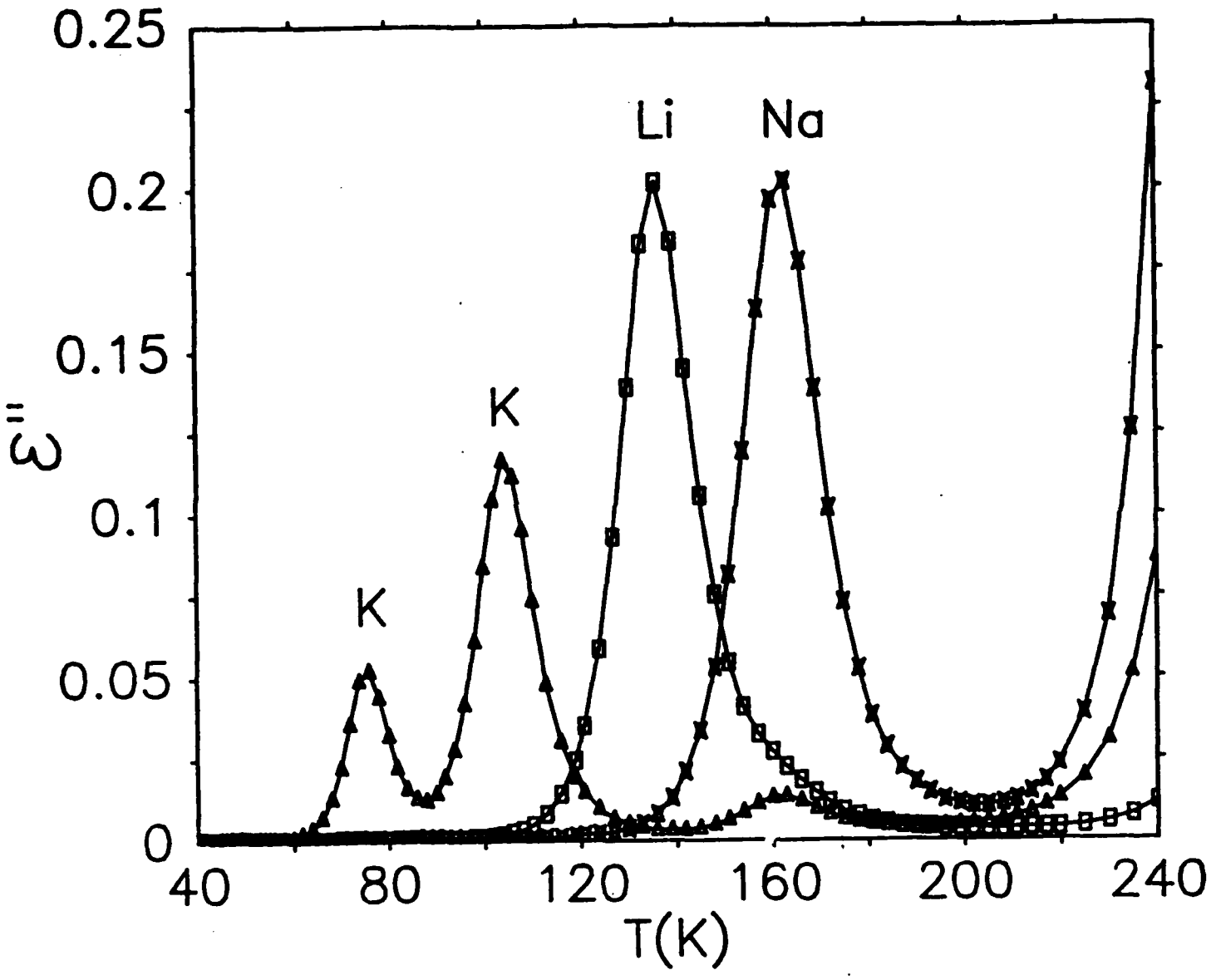

Fig. 5 - Favero et al.

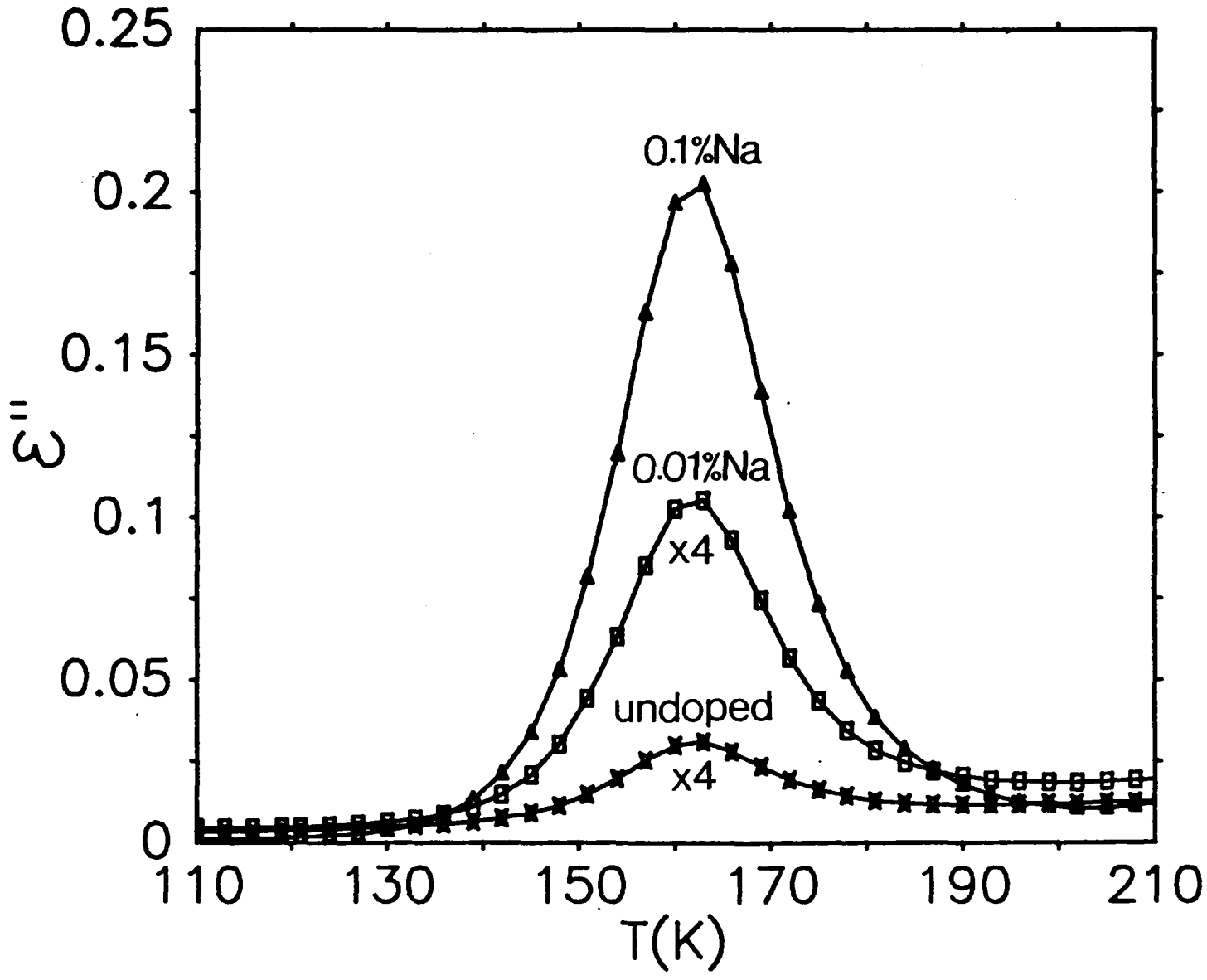
0.25
0.2
0.15
0.1
0.05
0
$\bar{\omega}$
0.1%Na
0.01%Na
x4
undoped
x4
110
130
150
170
190
210
T(K)

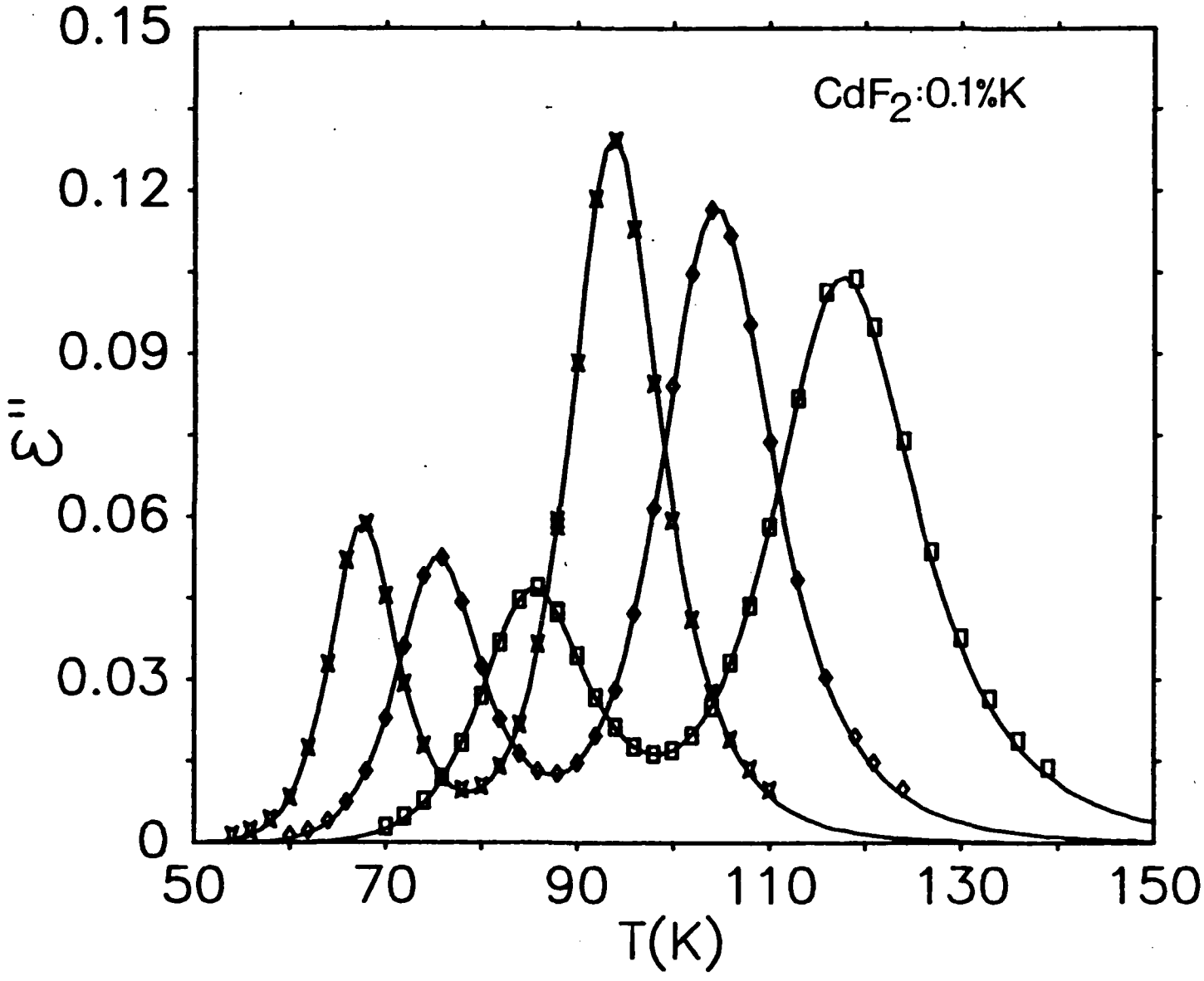

Fig.7 - Figueroa et al

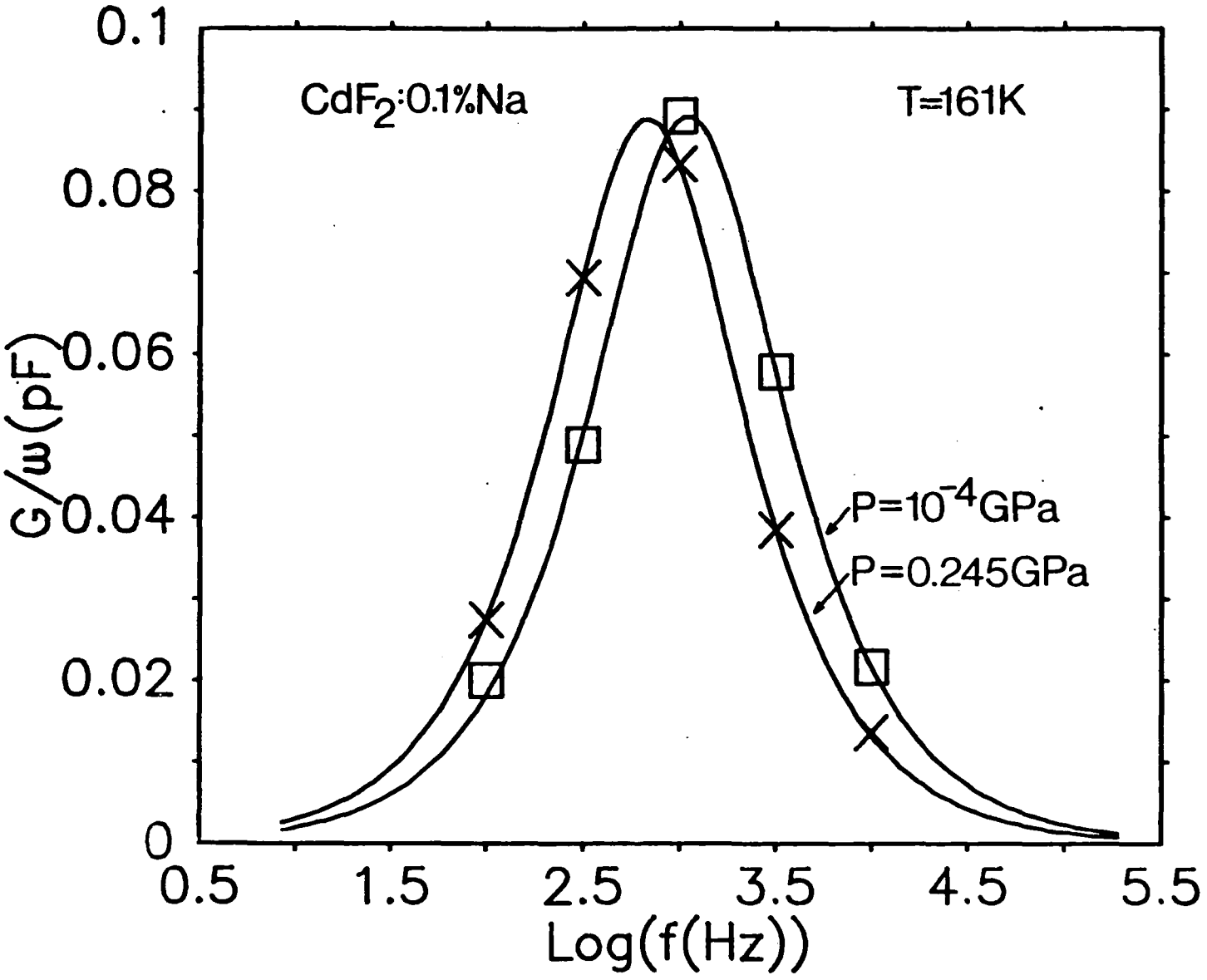

Fig. 8 - Figueroa et al

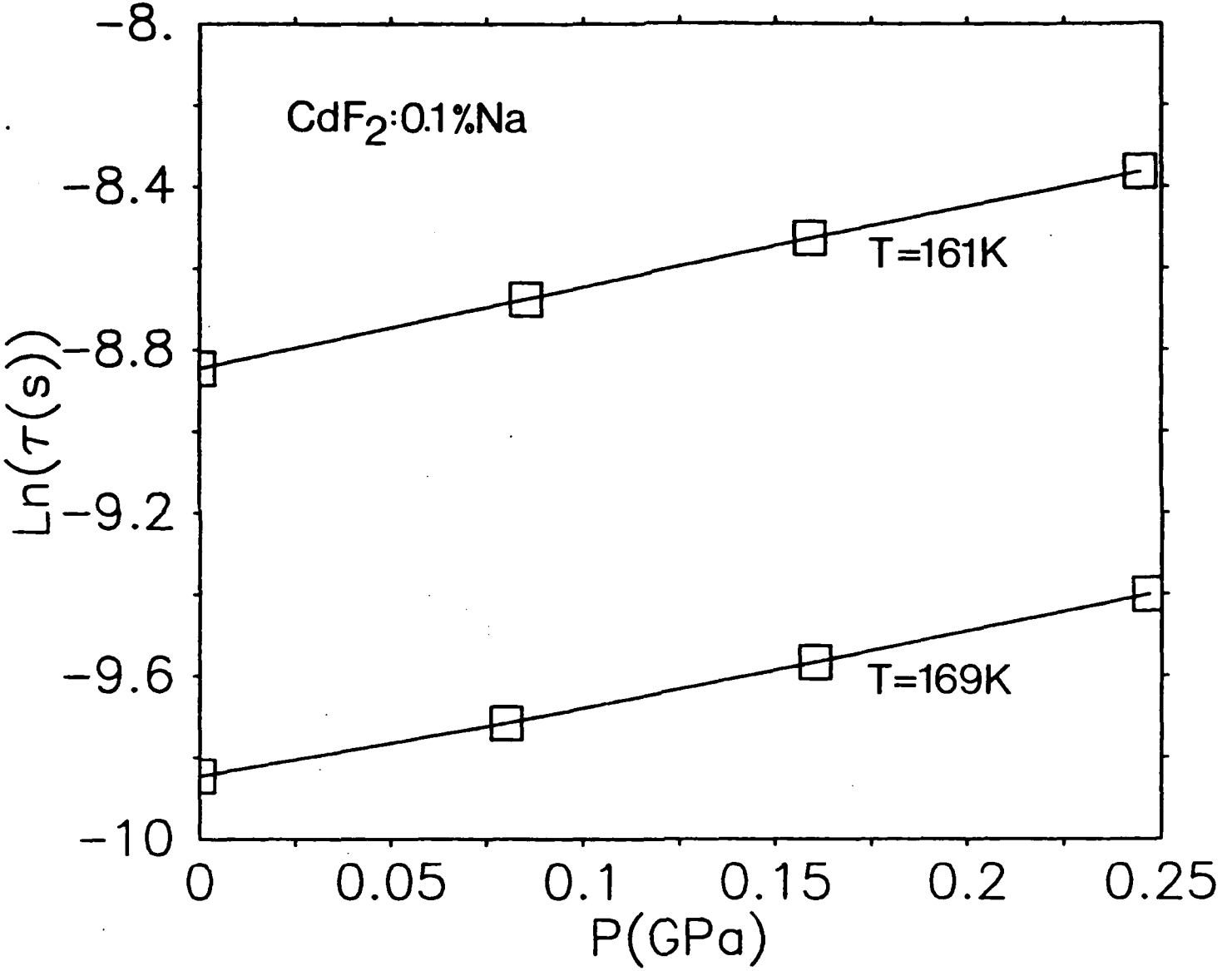
CdF2:0.1%Na
T=161K
T=169K
-8.
-8.4
-8.8
-9.2
-9.6
-10
Ln(τ(s))
0
0.05
0.1
0.15
0.2
0.25
P(GPa)

DL/413/83/01
GEN/413-2

TECHNICAL REPORT DISTRIBUTION LIST, GEN

	No. Copies
Office of Naval Research Attn: Code 413 800 N. Quincy Street Arlington, Virginia 22217	2
ONR Pasadena Detachment Attn: Dr. R. J. Marcus 1030 East Green Street Pasadena, California 91106	1
Commander, Naval Air Systems Command Attn: Code 310C (H. Rosenwasser) Washington, D.C. 20360	1
Naval Civil Engineering Laboratory Attn: Dr. R. W. Drisko Port Hueneme, California 93401	1
Superintendent Chemistry Division, Code 6100 Naval Research Laboratory Washington, D.C. 20375	1
Defense Technical Information Center Building 5, Cameron Station Alexandria, Virginia 22314	12
DTNSRDC Attn: Dr. G. Bosmajian Applied Chemistry Division Annapolis, Maryland 21401	1
Naval Ocean Systems Center Attn: Dr. S. Yamamoto Marine Sciences Division San Diego, California 91232	1
Naval Ocean Systems Center Attn: Technical Library San Diego, California 92152	1
Naval Weapons Center Attn: Dr. A. B. Amster Chemistry Division China Lake, California 93555	1
Scientific Advisor Commandant of the Marine Corps Code RD-1 Washington, D.C. 20380	1
Dean William Tolles Naval Postgraduate School Monterey, California 93940	1
U.S. Army Research Office Attn: CRD-AA-IP P.O. Box 12211 Research Triangle Park, NC 27709	1
Mr. Vincent Schaper DTNSRDC Code 2830 Annapolis, Maryland 21402	1
Mr. John Boyle Materials Branch Naval Ship Engineering Center Philadelphia, Pennsylvania 19112	1
Mr. A. M. Anzalone Administrative Librarian PLASTEC/ARRADCOM Bldg 3401 Dover, New Jersey 07801	1

DL/413/83/01
359/413-2

TECHNICAL REPORT DISTRIBUTION LIST, 359

Dr. Paul Delahay
Department of Chemistry
New York University
New York, New York 10003

Dr. P. J. Hendra
Department of Chemistry
University of Southampton
Southampton SO9 5NH
United Kingdom

Dr. T. Katan
Lockheed Missiles and
Space Co., Inc.
P.O. Box 504
Sunnyvale, California 94088

Dr. D. N. Bennion
Department of Chemical Engineering
Brighma Young University
Provo, Utah 84602

Dr. R. A. Marcus
Department of Chemistry
California Institute of Technology
Pasadena, California 91125

Mr. Joseph McCartney
Code 7121
Naval Ocean Systems Center
San Diego, California 92152

Dr. J. J. Auborn
Bell Laboratories
Murray Hill, New Jersey 07974

Dr. Joseph Singer, Code 302-1
NASA-Lewis
21000 Brookpark Road
Cleveland, Ohio 44135

Dr. P. P. Schmidt
Department of Chemistry
Oakland University
Rochester, Michigan 48063

Dr. H. Richtol
Chemistry Department
Rensselaer Polytechnic Institute
Troy, New York 12181

Dr. E. Yeager
Department of Chemistry
Case Western Reserve University
Cleveland, Ohio 44106

Dr. C. E. Mueller
The Electrochemistry Branch
Naval Surface Weapons Center
White Oak Laboratory
Silver Spring, Maryland 20910

Dr. Sam Perone
Chemistry & Materials
Science Department
Lawrence Livermore National Lab.
Livermore, California 94550

Dr. Royce W. Murray
Department of Chemistry
University of North Carolina
Chapel Hill, North Carolina 27514

Dr. G. Goodman
Johnson Controls
5757 North Green Bay Avenue
Milwaukee, Wisconsin 53201

Dr. B. Brummer
EIC Incorporated
111 Chapel Street
Newton, Massachusetts 02158

Dr. Adam Heller
Bell Laboratories
Murray Hill, New Jersey 07974

Electrochimica Corporation
Attn: Technical Library
2485 Charleston Road
Mountain View, California 94040

Library
Duracell, Inc.
Burlington, Massachusetts 01803

Dr. A. B. Ellis
Chemistry Department
University of Wisconsin
Madison, Wisconsin 53706

DL/413/83/01
359/413-2

TECHNICAL REPORT DISTRIBUTION LIST, 359

Dr. M. Wrighton
Chemistry Department
Massachusetts Institute
of Technology
Cambridge, Massachusetts 02139

Dr. B. Stanley Pons
Department of Chemistry
University of Utah
Salt Lake City, Utah 84112

Donald E. Mains
Naval Weapons Support Center
Electrochemical Power Sources Division
Crane, Indiana 47522

S. Ruby
DOE (STOR)
M.S. 6B025 Forrestal Bldg.
Washington, D.C. 20595

Dr. A. J. Bard
Department of Chemistry
University of Texas
Austin, Texas 78712

Dr. Janet Osteryoung
Department of Chemistry
State University of New York
Buffalo, New York 14214

Dr. Donald W. Ernst
Naval Surface Weapons Center
Code R-33
White Oak Laboratory
Silver Spring, Maryland 20910

Mr. James R. Moden
Naval Underwater Systems Center
Code 3632
Newport, Rhode Island 02840

Dr. Bernard Spielvogel
U.S. Army Research Office
P.O. Box 12211
Research Triangle Park, NC 27709

Dr. William Ayers
ECD Inc.
P.O. Box 5357
North Branch, New Jersey 08876

Dr. M. M. Nicholson
Electronics Research Center
Rockwell International
3370 Miraloma Avenue
Anaheim, California

Dr. Michael J. Weaver
Department of Chemistry
Purdue University
West Lafayette, Indiana 47907

Dr. R. David Rauh
EIC Corporation
111 Chapel Street
Newton, Massachusetts 02158

Dr. Aaron Wold
Department of Chemistry
Brown University
Providence, Rhode Island 02192

Dr. Martin Fleischmann
Department of Chemistry
University of Southampton
Southampton SO9 5NH ENGLAND

Dr. R. A. Osteryoung
Department of Chemistry
State University of New York
Buffalo, New York 14214

Dr. Denton Elliott
Air Force Office of Scientific
Research
Bolling AFB
Washington, D.C. 20332

Dr. R. Nowak
Naval Research Laboratory
Code 6130
Washington, D.C. 20375

Dr. D. F. Shriver
Department of Chemistry
Northwestern University
Evanston, Illinois 60201

Dr. Aaron Fletcher
Naval Weapons Center
Code 3852
China Lake, California 93555

DL/413/83/01
359/413-2

TECHNICAL REPORT DISTRIBUTION LIST, 359

Dr. David Aikens
Chemistry Department
Rensselaer Polytechnic Institute
Troy, New York 12181

Dr. A. P. B. Lever
Chemistry Department
York University
Downsview, Ontario M3J1P3

Dr. Stanislaw Szpak
Naval Ocean Systems Center
Code 6343, Bayside
San Diego, California 95152

Dr. Gregory Farrington
Department of Materials Science
and Engineering
University of Pennsylvania
Philadelphia, Pennsylvania 19104

M. L. Robertson
Manager, Electrochemical
and Power Sources Division
Naval Weapons Support Center
Crane, Indiana 47522

Dr. T. Marks
Department of Chemistry
Northwestern University
Evanston, Illinois 60201

Dr. Micha Tomkiewicz
Department of Physics
Brooklyn College
Brooklyn, New York 11210

Dr. Lesser Blum
Department of Physics
University of Puerto Rico
Rio Piedras, Puerto Rico 00931

Dr. Joseph Gordon, II
IBM Corporation
K33/281
5600 Cottle Road
San Jose, California 95193

Dr. D. H. Whitmore
Department of Materials Science
Northwestern University
Evanston, Illinois 60201

Dr. Alan Bewick
Department of Chemistry
The University of Southampton
Southampton, SO9 5NH ENGLAND

Dr. E. Anderson
NAVSEA-56Z33 NC #4
2541 Jefferson Davis Highway
Arlington, Virginia 20362

Dr. Bruce Dunn
Department of Engineering &
Applied Science
University of California
Los Angeles, California 90024

Dr. Elton Cairns
Energy & Environment Division
Lawrence Berkeley Laboratory
University of California
Berkeley, California 94720

Dr. D. Cipris
Allied Corporation
P.O. Box 3000R
Morristown, New Jersey 07960

Dr. M. Philpott
IBM Corporation
5600 Cottle Road
San Jose, California 95193

Dr. Donald Sandstrom
Department of Physics
Washington State University
Pullman, Washington 99164

Dr. Carl Kannewurf
Department of Electrical Engineering
and Computer Science
Northwestern University
Evanston, Illinois 60201

DL/413/83/01
359/413-2

TECHNICAL REPORT DISTRIBUTION LIST, 359

Dr. Robert Somoano
Jet Propulsion Laboratory
California Institute of Technology
Pasadena, California 91103

Dr. Johann A. Joebstl
USA Mobility Equipment R&D Command
DRDME-EC
Fort Belvoir, Virginia 22060

Dr. Judith H. Ambrus
NASA Headquarters
M.S. RTS-6
Washington, D.C. 20546

Dr. Albert R. Landgrebe
U.S. Department of Energy
M.S. 6B025 Forrestal Building
Washington, D.C. 20595

Dr. J. J. Brophy
Department of Physics
University of Utah
Salt Lake City, Utah 84112

Dr. Charles Martin
Department of Chemistry
Texas A&M University
College Station, Texas 77843

Dr. H. Tachikawa
Department of Chemistry
Jackson State University
Jackson, Mississippi 39217

Dr. Theodore Beck
Electrochemical Technology Corp.
3935 Leary Way N.W.
Seattle, Washington 98107

Dr. Farrell Lytle
Boeing Engineering and
Construction Engineers
P.O. Box 3707
Seattle, Washington 98124

Dr. Robert Gotscholl
U.S. Department of Energy
MS G-226
Washington, D.C. 20545

Dr. Edward Fletcher
Department of Mechanical Engineering
University of Minnesota
Minneapolis, Minnesota 55455

Dr. John Fontanella
Department of Physics
U.S. Naval Academy
Annapolis, Maryland 21402

Dr. Martha Greenblatt
Department of Chemistry
Rutgers University
New Brunswick, New Jersey 08903

Dr. John Wasson
Syntheco, Inc.
Rte 6 - Industrial Pike Road
Gastonia, North Carolina 28052

Dr. Walter Roth
Department of Physics
State University of New York
Albany, New York 12222

Dr. Anthony Sammells
Eltron Research Inc.
710 E. Ogden Avenue #108
Naperville, Illinois 60540

Dr. W. M. Risen
Department of Chemistry
Brown University
Providence, Rhode Island 02192

Dr. C. A. Angell
Department of Chemistry
Purdue University
West Lafayette, Indiana 47907

Dr. Thomas Davis
Polymer Science and Standards
Division
National Bureau of Standards
Washington, D.C. 20234

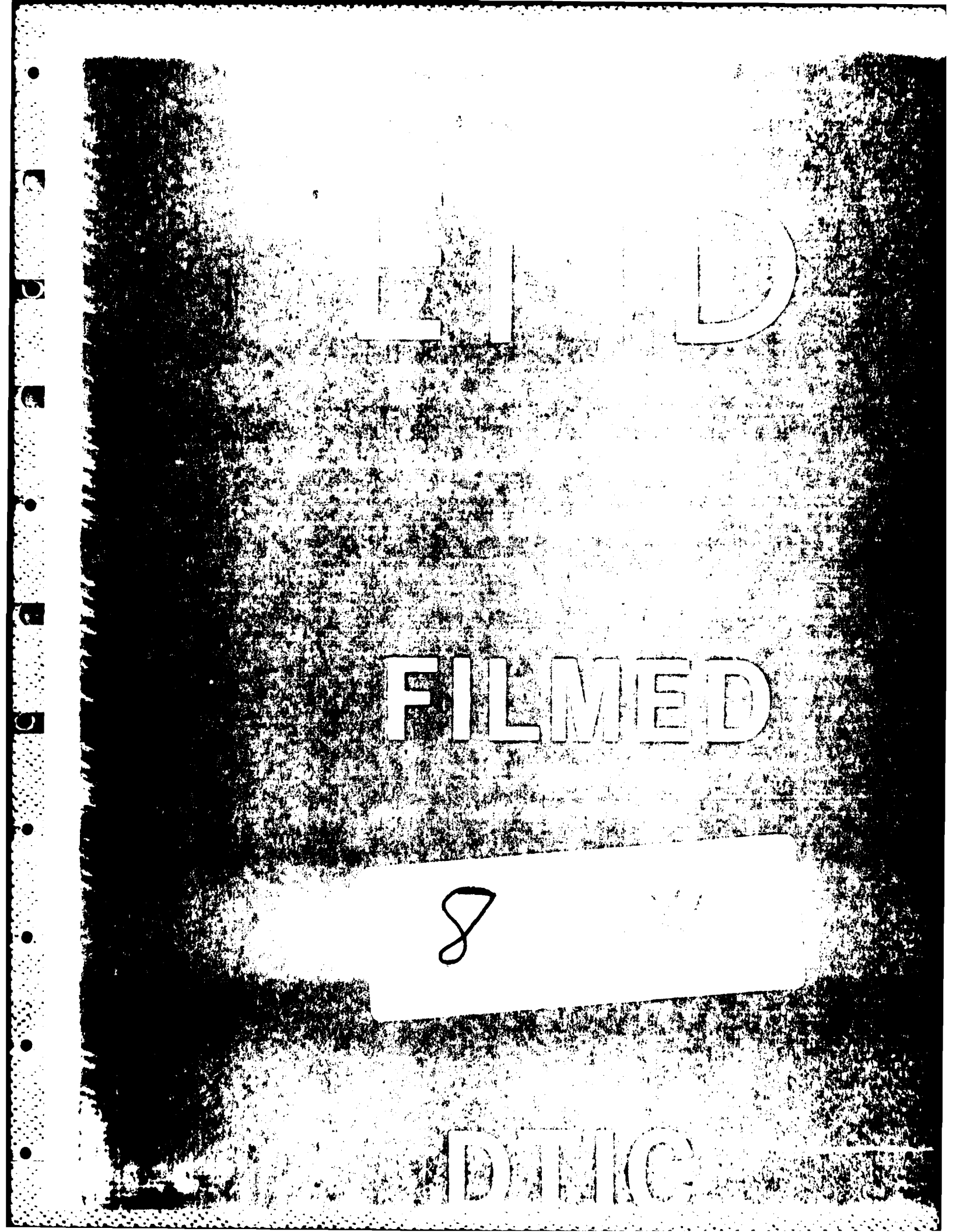
FILMED
8
DTIC